

A Numerical Investigation of Immiscible Two-Phase Fluid Flow Behaviour In Square and Circular Curved Ducts

T.T. Chandratilleke¹ and N. Nadim

¹Department of Mechanical Engineering
 Curtin University, Western Australia 6845, Australia

Abstract

Fluid flow within curved ducts is intrinsically subjected to centrifugal body forces induced by duct curvature and is characterised by the secondary flow vortex motion thus generated. For flow comprising non-mixing fluid components through curved ducts, the implications of secondary flow vastly differ from those on single-phase fluids or two-phase bubbly flows. Such flows develop complex flow dynamics due to differential phase fluid properties and phase velocities, and exchange momentum and heat across phase boundaries without any mass transfer. This study presents a numerical simulation that captures unique features of a two-component immiscible fluid flowing in a heated curved duct. Based on VOF approach, a multi-phase model is formulated for this flow under steady, turbulent and incompressible fluid conditions. The analysis examines the phase distribution and flow characteristics as influenced by duct curvature for both square and circular curved ducts. Unique flow features are identified and physically interpreted through the phase interactions and vortex structures.

Introduction

Flow of immiscible fluid mixtures often occur in many industrial applications. Some examples are: the crude oil transportation in oil and gas industry, chemical mixtures within reactors in pharmaceutical processes [1] and the mixtures of refrigerant and lubricant flow in refrigeration systems [2, 3].

The flow behaviour of immiscible fluid mixtures is fundamentally different to both single phase fluids and two-phase flow boiling. Flow dynamics of such fluids depend on the relative difference in phase fluid properties and phase velocities. Unique to immiscible fluids, the exchange of momentum and heat between phases occurs without any mass transfer. These flow attributes are accentuated when immiscible fluid mixtures flow through curved ducts.

In curved ducts, fluid flows are intrinsically subjected to centrifugal forces induced by duct curvature. These forces drive the fluid radially outwards creating a vortex motion known as secondary flow that typifies the curved duct flow characteristics.

When immiscible fluids flow in curved ducts, the centrifugal effects from duct curvature displace the heavier fluid component radially outwards. Consequently, fluid phases in the mixture are redistributed altering the interfacial area between phases and the flow regimes. Resulting flow patterns, phase separation, pressure drop and heat transfer characteristics are uniquely different to other types of fluid flows. Hence, a clearer understanding of immiscible flow behaviour is vitally important for developing new analytical tools for designing industrial equipment involving non-mixing fluids.

Fluid and thermal characteristics of single phase fluids in curved ducts have been relatively well explored in published literature. As key contributors to current knowledge, Chandratilleke et al.

[4-7] have performed a series of experimental and numerical work on heated curved ducts with extensive parametric results and simulation models on many duct geometries. Based on helicity, they recently reported a three-dimensional model [6] that is regarded to be the most accurate to-date, with novel vortex detection techniques. This advanced model has been successfully extended to two-phase flow boiling in curved pipes [7].

Much research on immiscible fluid mixtures has been confined to straight ducts, where studies typically examine the phase instability arising from the viscosity differences and, fluid and thermal characteristics [8,9]. To the contrary, many fundamental aspects of immiscible fluid mixture flow in curved ducts still remain unexplored in spite of significant process industry applications. In accounting for these, the analysis presented in this paper examines the unique flow behaviour associated with immiscible fluid mixtures within curved ducts. It evaluates the development of secondary flow within fluid phases, phase redistribution arising from duct curvature and the associated thermal and fluid flow features.

Numerical Model

The numerical model is formulated for a semicircular curved duct of fixed radius, as shown in Fig. 1 along with the dimensions used. The analysis considers square and circular ducts having a hydraulic diameter of 10 mm.

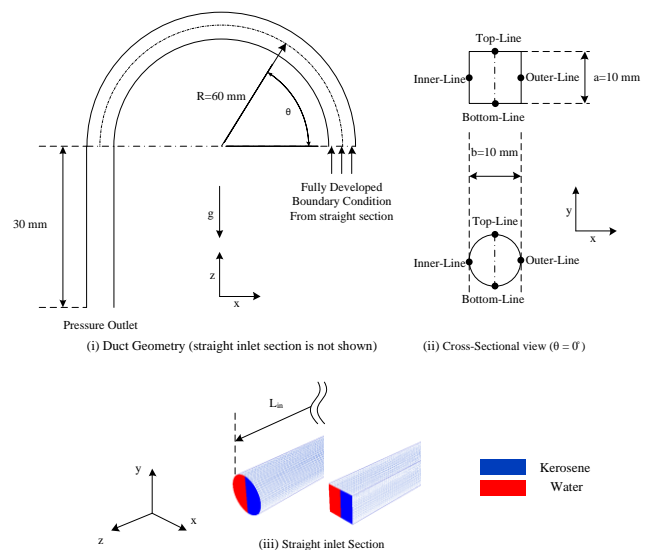


Fig. 1 Model configuration with geometrical parameters

The immiscible working fluid is taken to be a mixture of water (Phase 1) and kerosene (Phase 2), which is fed to the curved duct through a straight inlet duct to ensure fully-developed conditions at the curved duct entry. The flow rates of fluid phases are independently varied to examine influence of velocity ratio on

phase and flow pattern. Among investigated cases, inlet velocity ratio is 1 for Case-B where both phases' inlet velocity is maximized on 1 m/s. For Case A and B, velocity of higher flow rate phase is kept at one and inlet velocity of eased phase is reduced to 0.25 m/s in order to achieve mentioned velocity ratios. Pressure outlet boundary condition is applied at the flow exit.

Governing equations

The model is based on Volume of Fraction (VOF) approach enhanced by using the Level-Set method [10] for improved phase boundary tracking. The interface is implicitly represented by the level set of $\varphi(x) = 0$ that is defined by,

$$\varphi(x) = \begin{cases} +|d_{interface}| & x \in \text{Phase-1} \\ 0 & x \in \Gamma \\ -|d_{interface}| & x \in \text{Phase-2} \end{cases} \quad 1$$

where, Γ represents interface area and $d_{interface}$ is cell distance from interface. Conservation of Level Set function is given by,

$$\nabla \cdot (\vec{u}\varphi) = 0 \quad 2$$

Accounting for phase effects with the equivalent bulk density, the continuity equation is given by,

$$\nabla \cdot (\rho_m \vec{u}) = 0 \quad 3$$

Taking subscript "k" to denote each phase, bulk values for a cell are described by,

$$\rho_m = \sum_k \alpha_k \rho_k \quad 4(a)$$

$$4(b)$$

$$\mu_m = \sum_k \alpha_k \mu_k$$

The momentum equations coupled with Level-Set are derived as,

$$\vec{u} \cdot \nabla (\rho_m \vec{u}) = -\nabla p + \mu_m (\nabla^2 \vec{u} + \nabla^2 \vec{u}^T) - \alpha \kappa \delta(\varphi) + \rho_m \vec{g} + \vec{F}_c \quad 5(a)$$

$$\delta(\varphi) = \begin{cases} \frac{1 + \cos(\pi\varphi/1.5gs)}{3gs} & |\varphi| \leq 1.5gs \\ 0 & |\varphi| > 1.5gs \end{cases} \quad 5(b)$$

where gs is grid spacing size. Turbulence effects are included as ($k-\omega$) model [11], where turbulence kinetic energy k and specific dissipation rate ω are obtained from the closures as:

Kinematic Eddy viscosity:

$$\nu_\tau = \frac{k}{\omega}, \quad \tilde{\omega} = \max\left\{\omega, C_{lim} \sqrt{\frac{2S_{ij}S_{ij}}{\beta^*}}\right\}, \quad C_{lim} = \frac{7}{8} \quad 6$$

Turbulence Kinetic energy:

$$u_j \frac{\partial k}{\partial x_j} = \tau_{ij} \frac{\partial u_i}{\partial x_j} - \beta^* k \omega + \frac{\partial}{\partial x_j} \left[(\nu + \sigma^* \frac{k}{\omega}) \frac{\partial k}{\partial x_j} \right] \quad 7$$

Specific dissipation rate:

$$u_j \frac{\partial \omega}{\partial x_j} = \alpha \frac{\omega}{k} \tau_{ij} \frac{\partial u_i}{\partial x_j} - \beta \omega^2 + \frac{\sigma_d}{\omega} \frac{\partial k}{\partial x_j} \frac{\partial \omega}{\partial x_j} + \frac{\partial}{\partial x_j} \left[(\nu + \sigma \frac{k}{\omega}) \frac{\partial \omega}{\partial x_j} \right] \quad 8$$

Closure coefficients and auxiliary relations are:

$$\alpha = \frac{13}{25}, \quad \beta = \beta_o f_\beta, \quad \beta^* = \frac{9}{10}, \quad \sigma = \frac{1}{2}, \quad \sigma^* = \frac{3}{5}, \quad \sigma_d = \frac{1}{8} \quad 9$$

$$\beta_o = 0.0708, \quad f_\beta = \frac{1 + 85\chi_\omega}{1 + 100\chi_\omega}, \quad \chi_\omega = \frac{|\Omega_y \Omega_x S_{ij}|}{(\beta^* \omega)^2} \quad 10$$

$$\Omega_y = \frac{1}{2} \left(\frac{\partial u_i}{\partial x_j} - \frac{\partial u_j}{\partial x_i} \right), \quad S_{ij} = \frac{1}{2} \left(\frac{\partial u_i}{\partial x_j} + \frac{\partial u_j}{\partial x_i} \right) \quad 11$$

Dimensionless Helicity function is defined for each phase according to its material properties and reference values, and is given for phase "p" by,

$$H_k^* = \alpha_k \cdot H \cdot D_h \frac{v}{v_{ref}} \frac{1}{U^2_{in-k}}$$

This permits clear identification of vortex structure within fluid phases by defining an appropriate threshold for H_p^* such as 0.01 that is consistently used in the current analysis.

Results and Discussion

Fig. 2 depicts the volume fraction distribution of fluid phase in the immiscible mixture along square and circular curved ducts from inlet ($\theta = 0^\circ$) to outlet ($\theta = 180^\circ$). The red and blue contours respectively indicate Phase 1 (heavier) and Phase 2 (lighter) while the right side of figure indicates outer duct wall.

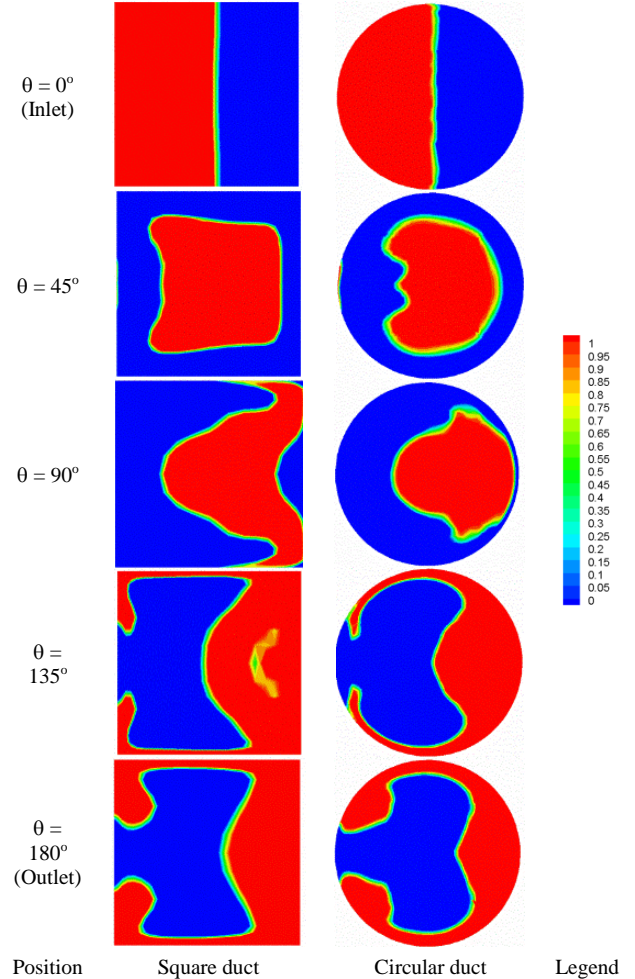


Fig. 2 Volume of fraction contours depicting phase distribution at various duct cross sections (Phase velocity ratio = 1.0)

At inlet ($\theta = 0^\circ$), Phase 1 enters the duct attached to the inner wall while Phase 2 flows closer to the outer wall. The interfacial boundary between the two phases is practically a straight line for both types of ducts.

As the immiscible mixture flows through the curved duct, it gradually experiences the centrifugal effects from duct curvature and consequently undergoes redistribution of fluid phases that is essentially determined by the dynamics of body forces acting on fluid elements. The centrifugal forces will have more inertial influence on the fluid phase with higher density (Phase 1). Consequently, this heavier fluid phase begins to migrate towards the outer wall, as illustrated in Fig. 2.

At ($\theta = 45^\circ$), the volume fraction contours show that, Phase 1 is in dynamic equilibrium in the duct centre surrounded by Phase 2. For positions $\theta = 90^\circ, 135^\circ, 180^\circ$, the centrifugal action keeps

moving Phase 1 towards the outer wall, gradually displacing the initial cushioning layer of Phase 2. In these phase distributions at mid-duct sections, Phase 1 flows closer to the outer wall while Phase 2 flows along the inner wall. These phase attributes are complete opposite to those at curved duct inlet and demonstrate the effect from duct curvature on immiscible fluid mixture flow characteristics.

Compared to other types of fluid flows, immiscible mixtures in curved ducts tend to have unique secondary flow behaviour. This is because the immiscible fluid components are subjected to simultaneous effects of momentum exchange between phases and the curvature-induced centrifugal action. The degree of influence from these actions varies depending on the phase density and viscosity values. In this, the centrifugal forces dominate the flow pattern of high-density phase while the high-viscosity phase regulates the momentum transfer between phases. The overall flow characteristics are determined by the relative strength of centrifugal and viscous forces operating on the fluid mixture.

In Fig. 3, typical flow patterns for the immiscible mixture are illustrated using the dimensionless helicity function defined by Eq. 12. The helicity distributions within each phase are given at selected curved duct sections for both square and circular geometries. In this, the red and blue contours are respectively for Phase 1 and Phase 2. The solid lines and dashed line respectively indicate the clockwise and counter-clockwise fluid rotations. The right side of figure denotes the outer duct wall.

As clearly evident in Fig. 3, the secondary flow patterns in immiscible mixtures are more complex and vastly different to those in single phase fluid flow in curved ducts. Each phase essentially behaves as a separate secondary flow cell within which vortices are formed and stagnation regions are developed. However, these secondary flow circulations are interconnected by viscous forces and undergo momentum exchange between them. Thus the adjacent vortex loops have opposing rotational directions within phases and across phase boundaries.

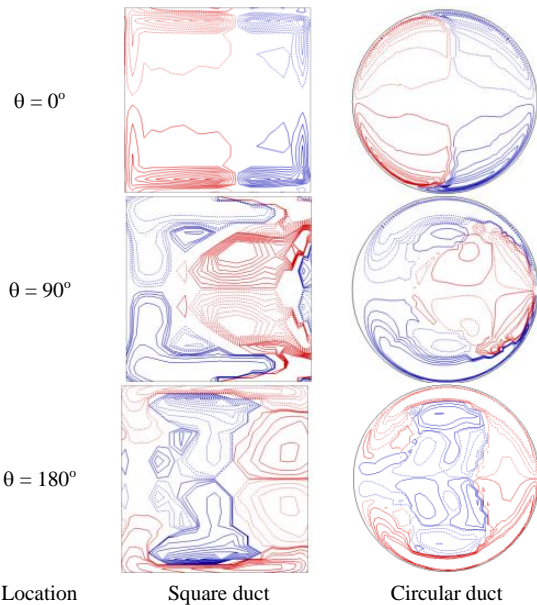


Fig. 3 Dimensionless helicity contours for immiscible flow (Phase velocity ratio = 1.0)

At inlet ($\theta = 0^\circ$), Fig. 3 shows the initial stage of secondary vortex formation within phase boundaries. At this stage, Phase 1 flows closer to the inner wall and the fluid circulations in each phase occur in the same corresponding direction at the top and the bottom half of duct cross section. As the fluid moves downstream ($\theta > 0^\circ$), it experiences centrifugal body forces that displace Phase 2 towards the inner wall, as shown at $\theta = 90^\circ$,

where regions of highly localised secondary vortices are observed. These vortices rotate in opposite directions indicating fluid momentum transfer between adjacent vortex cells. By the duct exit ($\theta = 180^\circ$), the momentum transfer from Phase 1 circulations become so dominant, it restricts the Phase 2 circulation practically to the centre of duct.

In appraising phase dominance, the flow situations are examined in Fig. 4 under three velocity combinations, namely Case (A), Case (B) and Case (C), where the ratios of Phase 1 to Phase 2 velocities are set at 0.25, 1.0 and 4.0, respectively. For these three cases, Fig. 4 depicts the phase distribution and the helicity patterns at the exit of both square and circular ducts.

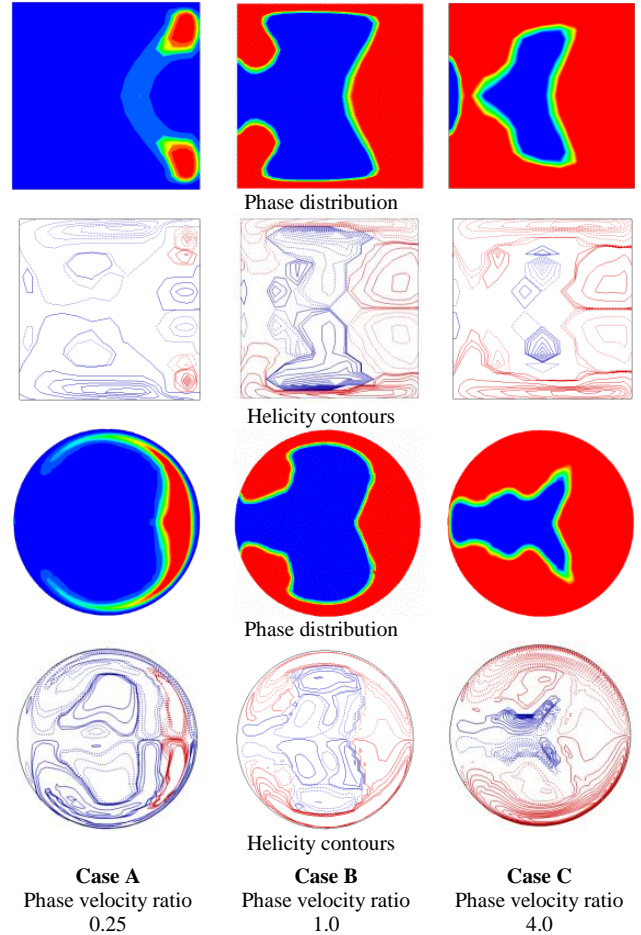


Fig. 4 Velocity ratio effect on phase distribution and secondary flow structures (contours at exit plane $\theta=180^\circ$)

It is observed that, although the heavier Phase 1 enters the curved channel attached to the inner wall, it gets displaced to the outer wall by the channel exit under the influence of centrifugal forces for all velocity ratios. At the low velocity ratio of 0.25, the bulk flow is occupied by strong secondary flow circulation in Phase 2. This circulation imparts momentum transfer on Phase 1 to set up localised Phase 1 circulations near the outer wall. Under these conditions, the flow patterns are dominated by momentum transfer from Phase 2 to Phase 1. As the velocity ratio is increased, the centrifugal forces emphasise the secondary flow circulation in Phase 1 because of its high density and lower dynamic viscosity compared to Phase 2. This causes the circulatory momentum of Phase 1 to act against and reverse the momentum flow from Phase 2. Consequently at increased velocity ratios, the bulk flow pattern begins to be dominated by Phase 1 circulation, as shown by Fig 4.

The interfacial area separating fluid phases is a crucial aspect for immiscible fluid components that react with each other, as in

chemical processing. In such cases, the maximised interfacial contact improves production efficiency. Fig. 5 shows the ratio of interfacial phase area for immiscible flow through curved duct (IA-Curved) to that in straight duct (IA-Straight) with the same length in terms of inlet velocity ratio.

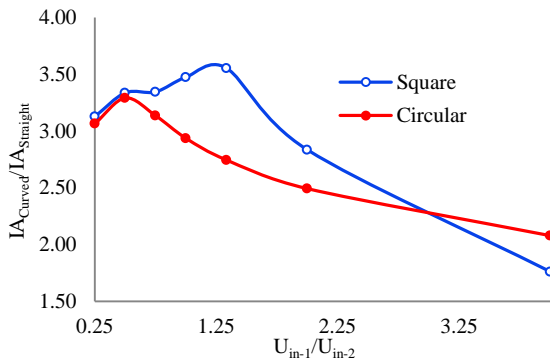


Fig. 5 Variation of phase interfacial area with velocity ratio

It is clearly evident that the immiscible flow in a curved duct provides more than 3 times interfacial area between phases compared to a straight duct. This shows the usefulness of the curved geometry in improving the reaction potential between phases although it may accompany a slight pressure loss penalty. A square curved duct is seen to provide up to 60 per cent more interfacial area compared to a circular channel at lower velocity ratios. For increasing velocity ratio, the interfacial area advantage gradually diminishes for both square and circular ducts along with higher pressure drop penalties.

Conclusions

The numerical model discussed in this paper accurately captures the unique features of two-phase immiscible fluid mixture flowing in circular curved ducts. The immiscible flow behaviour is essentially determined by the curvature-induced centrifugal forces and the viscous forces. The centrifugal forces drive the heavier fluid phase towards the outer duct wall and create secondary flow circulations within the immiscible fluid mixture. The viscous forces facilitate the transfer of secondary flow fluid momentum across phase boundaries leading to rotationally-connected secondary vortices in immiscible fluid phases. The dynamic equilibrium between centrifugal and viscous forces determine the unique attributes of phase distribution and flow patterns of immiscible mixture through curved ducts.

References

- [1] Wegmann, A., Rohr, P. R., Two phase liquid–liquid flows in pipes of small diameters, *International Journal of Multiphase Flow*, 32, 2006, 1017–1028.
- [2] Kruse, H. H. and Schroeder, M., Fundamentals of lubrication in refrigerating systems and heat pumps, *International Journal of Refrigerating*, 8, 1985.
- [3] Sunami, M., Takigawa, K., Suda, S., New Immiscible Refrigeration Lubricant for HFCs, *International Refrigeration and Air Conditioning Conference*, 1994.
- [4] Chandratilleke, T. T., Secondary flow characteristics and convective heat transfer in a curved rectangular duct with external heating, *5th World Conference On Experimental Heat Transfer, Fluid Mechanics and Thermodynamics*, Thessaloniki, Greece, 2001.
- [5] Chandratilleke, T. T. and Nursubyakto, Numerical prediction of secondary flow and convective heat transfer in externally heated curved rectangular ducts, *International Journal of Thermal sciences*, 42, 2002, 187–198.
- [6] Chandratilleke, T. T., Nadim, N., Narayanaswamy, R., Vortex structure-based analysis of laminar flow behaviour and thermal characteristics in curved ducts, *International Journal of Thermal Sciences*, 59, 2012, 75–86.
- [7] Chandratilleke, T. T., Nadim, N. and Narayanaswamy, R., An Investigation Of Flow Boiling With Secondary Flow Interaction In Curved Pipes, *ECI 8th International Conference on Boiling and Condensation Heat Transfer*, Ecole Polytechnique Fédérale de Lausanne, Lausanne, Switzerland, 2012.
- [8] Joseph, D. D., Renardy, M. and Renardy, Y., Instability of flow of two immiscible liquids with different viscosities in a pipe, *International Journal of Fluid Mechanics*, 141, 1984, 309–317.
- [9] Eastwood, C. D., Armi, L. , Lasheras, J. C., The breakup of immiscible fluids in turbulent flows, *International Journal of Fluid Mechanics*, 502, 2004, 309–333.
- [10] Olsson, E., Kreiss, G., A conservative level set method for two phase flow, *Journal of Computational Physics*, 210, 2005, 225–246.
- [11] Wilcox, D. C., *Turbulence Modeling for CFD (3rd Edition)*, DCW Industries Inc.A, 2010.